

Title	Morphological characterization of the peri-implant epithelium in vivo
Author(s)	Ishida, S; Matsuzaka, K; Itou, F; Kaketa, A; Kaneuchi, H; Endo, T; Inoue, T
Journal	日本口腔検査学会雑誌, 6(1): 50-57
URL	http://hdl.handle.net/10130/3298
Right	

Morphological characterization of the peri-implant epithelium *in vivo*

Ishida S¹⁾, Matsuzaka K^{1), 2)}, Itou F¹⁾, Kaketa A¹⁾, Kaneuchi H¹⁾, Endo T¹⁾, Inoue T^{1), 2)*}

1. Department of Clinical Pathophysiology, Tokyo Dental College

2. Oral Health Science center, Tokyo Dental College

Abstract

The purpose of this study was to investigate the morphological changes of the peri-implant epithelium (PIE) after implantation *in vivo*. A screw-shaped pure titanium implant (ITI) was inserted in the mandibles of dogs who were sacrificed 1 and 3 months later. Both sides of the mandibles with implants were removed and fixed and approximately 30 μ m grinding sections were then cut and stained with toluidine blue. The length of the PIE was measured (L-PIE) and the ratios of both the length and width of the PIE (RL-PIE, RW-PIE) were calculated in the sections. Morphologically, the PIE was classified into three groups; 1: wedge-type, which was similar to the attachment epithelium of the natural tooth and there was no significant difference in the RL-PIE between 1 and 3 months, 2: thick-type, which was similar to the wedge-type but the thickness was increased and the RL-PIE decreased with time, and 3: ridge-type, which had an epithelium with elongated rete ridges with inflammatory reactions of connective tissue and the RL-PIE decreased with time. The RW-PIE was thinnest in the wedge-type and thickest in the ridge-type in all measured areas. These results suggest that the PIE divides into three distinct types due to the degree of inflammation and eventually becomes stable.

Key words : dental implants, peri-implant epithelium, morphology, inflammation, *in vivo*

Resved : December 20th 2013 accepted : March 20th 2014

Introduction

Replacement therapy, in which a tissue or organ and synthetic materials coexist, has become a requisite for modern medical science. Even in the dentistry, the use of oral implants has grown extensively during the last 30 years because of the increased demand for dental care of patients who have lost their teeth. A systematic review also showed a high survival rate

of patients who have had replacement therapy¹⁾. The clinical success of replacement therapy rests on the formation of a stable interface between the tissue and the implant²⁾³⁾.

Formation of the interface between the host tissue and a titanium implant occurs during the process of wound healing. When a cavity is prepared in the bone for implantation, the cavity

* : 2-9-18 Misaki-cho, Chiyoda-ku, Tokyo, 101-0061 JAPAN

TEL: +81-3-6380-9252 FAX: +81-3-6380-9606

e-mail: inoue@tdc.ac.jp

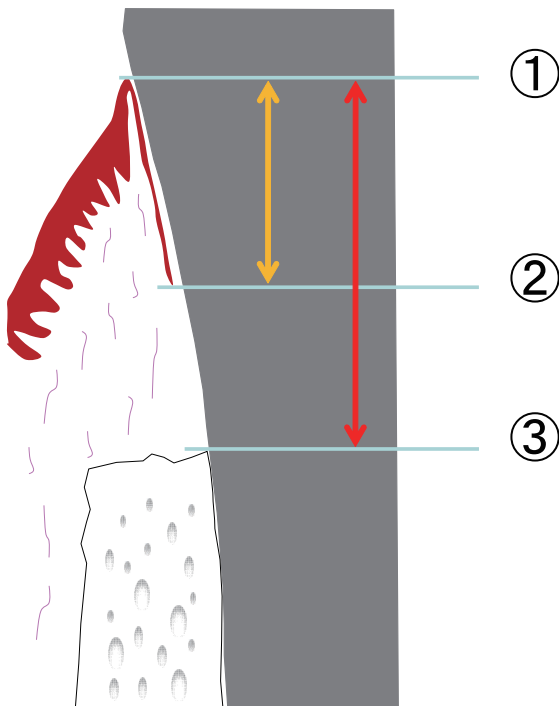


Fig. 1: L-PIE and RL-PIE
 The L-PIE is the length of the PIE.
 Fig.1-1 shows the top of the PIE and Fig. 1-2 shows the bottom of the PIE.
 The soft tissue length (STL) is from the top of the PIE to the bone surface (Fig. 1-3). The ratio of the peri-implant length (RL-PIE) was calculated according to the following formula:

$$RL-PIE = L-PIE / STL \times 100 (\%)$$

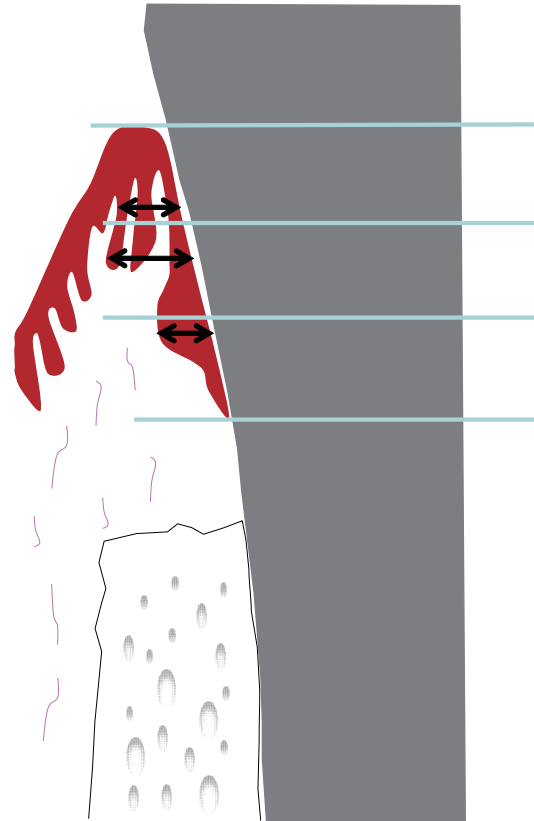


Fig. 1: L-PIE and RL-PIE
 Fig. 2: W-PIE
 The PIE is divided into three parts; top, middle and bottom areas. The width of the PIE in each of the parts was measured (mm).

initially fills with blood clots within several hours due to hemorrhaging and coagulation. Next, the blood clots are processed and removed during the inflammatory reaction, in which leukocytes clean up the damaged tissue debris and purge bacteria that have invaded the wound. After the cavity is cleaned up by this purification process, capillaries and fibroblasts invade into the wound area and prepare a stromal tissue for tissue restoration called granulation tissue. The remaining oral epithelium of the wound area migrates into the granulation tissue, and in the meantime, epithelial cells penetrate along the implant surface, and as a result, the peri-implant epithelium (PIE) is formed⁴⁾. However, the newly formed PIE is not a complete seal, and therefore, defense mechanisms by the PIE become an important point in terms of preventing bacterial invasion⁵⁾⁻

⁹⁾. There are defense factors in the junctional epithelium, i.e. bonding mechanical closures such as hemi-desmosomes, as well as proliferation capability and phagocytic activity of junctional epithelial cells¹⁰⁾¹¹⁾. However, only a few hemi-desmosomes were observed in small animals³⁾⁷⁾ and the presence of cytokeratin (CK) 19, which is expressed by immature and embryonic keratin-positive cells of the central and enamel side of the junctional epithelium, indicates strong proliferating activity but CK19 negativity of the PIE indicates a weak proliferating activity⁶⁾⁸⁾. Furthermore, dental implant therapy creates an open wound and an epithelium-implant interface, and that open wound is always exposed to the possibility of inflammation and/or infection¹²⁾.

However, details of the morphological changes around the dental implant after implantation,

particularly the PIE, in terms of length, width and type, have not been well investigated. The purpose of this paper was to investigate the morphological characterization of the PIE after implantation.

Materials and Methods

1. Animals

Four male 1.5 year old beagle dogs, each weighing approximately 10-12 kg, were used in this study. Throughout the experimental period, animals were fed kneaded food with water to avoid too much stress. Teeth and implants were brushed every 2 days during the experimental period. All experiments were performed according to the laboratory animal guidance of the Tokyo Dental College (approval number: 253206).

2. Anesthesia

The dogs were anesthetized using both ketamine hydrochloride (12.5 mg/kg, KET AL. AR® Daiichi-sankyo, Tokyo, Japan) and pentobarbital sodium (16.2 mg/kg, Somnopentyl®, Kyouritu-seiyaku, Tokyo, Japan), and local anesthesia was performed using lidocaine hydrochloride and epinephrine sodium (1.8 ml, Xilestesin®, 3M Sumitomo, Tokyo, Japan)

3. Surgical procedure

The premolar teeth on both sides of each mandible were extracted and wound healing was allowed for 3 months. A muco-periosteal flap was raised to expose both the buccal and lingual alveolar bones and then a screw-shaped pure titanium implant (ITI monotype implants, SLA surface, 4 mm in diameter, 8 μ m in length, Strauman Basel, Switzerland), which has a milled polished surface of the neck region, was inserted in the healed mandibular. Each dog received 6 implants and thus there was a total of 24 implants for all 4 dogs.

4. Histological Procedure

Two dogs at each time point were sacrificed by an overdose of pentobarbital sodium at 1 and 3 months after the implantation. Both sides of the mandibles with implants were removed and fixed in 10% neutral buffered formalin for 1 week at room temperature. Each mandible bone with an implant was cut using a diamond saw and made into small pieces. Twelve implants at each of the time periods were used for evaluation.

5. Grinding sections

The samples were washed with running water and

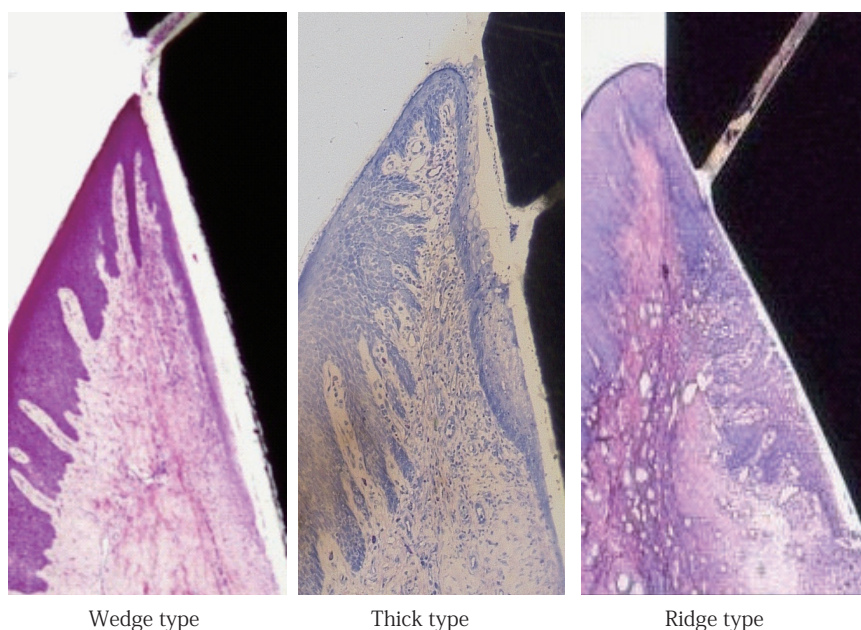


Fig. 3: Histological Classification Types of PIE

dehydrated with graded ethanol before embedding in MMA resin. Approximately 30 μ m sections were cut using a saw microtome (LEITZ1600SP, Leica, Wetzlar, Germany) and the surface of each section was then polished and stained with toluidine blue at pH 4. 0 and was then observed using a light microscope. Calculations were performed as follows:

1) Length of the PIE (L-PIE)

From the top (Fig. 1- ①) to the bottom (Fig. 1- ②) of the PIE was measured as the L-PIE (mm).

2) Ratio of the PIE (RL-PIE)

From the top of the PIE (Fig. 1- ①) to the bone surface (Fig. 1- ③) was measured as the soft tissue length (STL), and the RL-PIE was calculated according to the formula:

$$RL-PIE = \frac{L-PIE}{STL} \times 100 (\%)$$

3) Width of the PIE (W-PIE).

The PIE was divided into three equal parts (Fig. 2); top area, middle area and bottom area. The width of the PIE of the central part at each of the areas was measured as the W-PIE (mm).

6. Statistical analysis

The data were analyzed using Student's t test.

Results

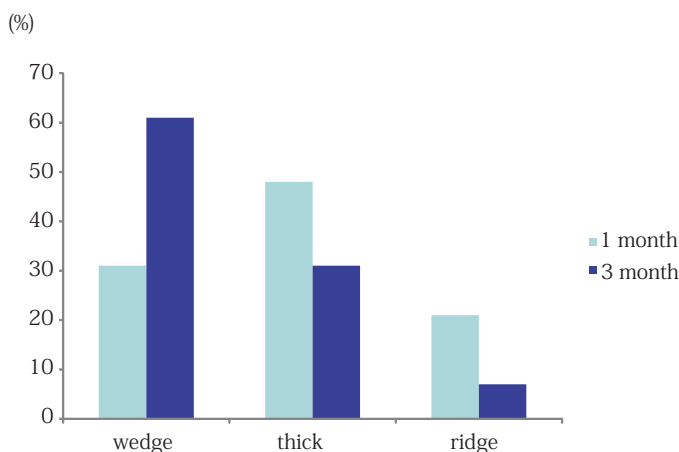
1. Histopathological observations

Implant-tissue interfaces consisted of three parts: the implant-epithelium interface which makes the PIE, the implant-connective tissue interface and the implant-bone interface. The PIE was morphologically classified into three groups; wedge-type, thick-type and ridge-type (Fig. 3).

The wedge-type, which was similar to the attachment epithelium of natural teeth, was thickest at the top area and thinnest at the bottom area which made a wedge-like shape. In the connective tissue underneath the epithelium of the wedge-type, a uniformly dense collagen fiber meshwork directly supported the PIE. There were no signs of acute inflammation or chronic cell infiltration.

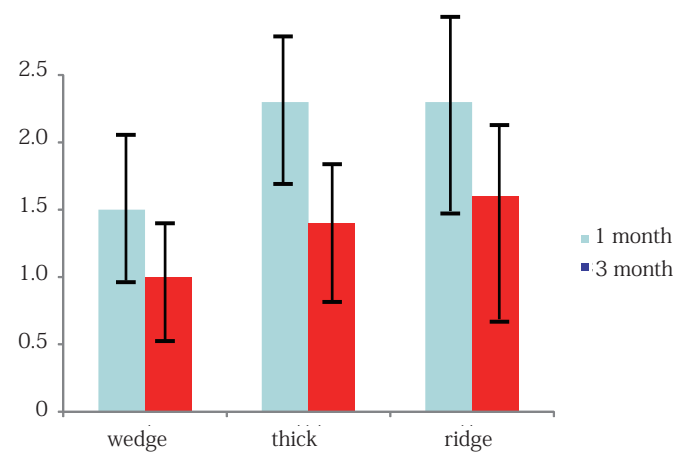
The thick-type had an increased width of the PIE at all areas. In the connective tissue underneath the epithelium, there were a number of small round infiltrating cells mainly consisting of lymphocytes.

The ridge-type had elongated rete ridges. The PIE was relatively thick and there were many



	1 month	3 months
wedge	31%	61%
thick	48%	31%
ridge	21%	7%

Fig. 4: Ratio of PIE type
The wedge-type was 31% at 1 month, and 61% at 3 months. The thick-type was 48% at 1 month and 31% at 3 months. The ridge-type was 21% at 1 month, and 7% at 3 months.



	1 month	3 months	P<0.05
wedge	1.5 ± 0.6	1.0 ± 0.4	*
thick	2.3 ± 0.6	1.4 ± 0.5	*
ridge	2.3 ± 0.7	1.6 ± 0.7	*

Fig.5: Length of the PIE (L-PIE: mm)

lymphocytes and plasma cells and a sparse and random orientation of collagen fibers in the connective tissue underneath the PIE and elongation of rete ridges in the connective tissues were observed.

2. Histomorphometric analysis of the PIE

1) Type of PIE (Fig. 4)

The wedge-type was 31% at 1 month and 61% at 3 months; the thick-type was 48% at 1 month and 31% at 3 months; and the ridge-type was 21% at 1 month and 7% at 3 months. The wedge-type increased with time whereas both the thick- and ridge-types decreased with time.

2) L-PIE (Fig. 5)

The L-PIE of the wedge-type was 1.5 ± 0.6 mm at 1 month and 1.0 ± 0.4 mm at 3 months. The L-PIE of the thick-type was 2.3 ± 0.6 mm at 1 month and 1.4 ± 0.5 mm at 3 months. The L-PIE of the ridge-type was 2.3 ± 0.7 mm at 1 month and 1.6 ± 0.7 mm at

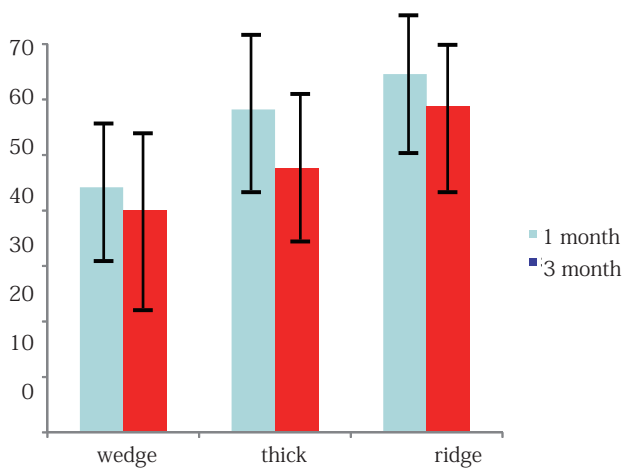
3 months. The L-PIE decreased with time at all time periods ($P < 0.05$).

3) RL-PIE (Fig. 6)

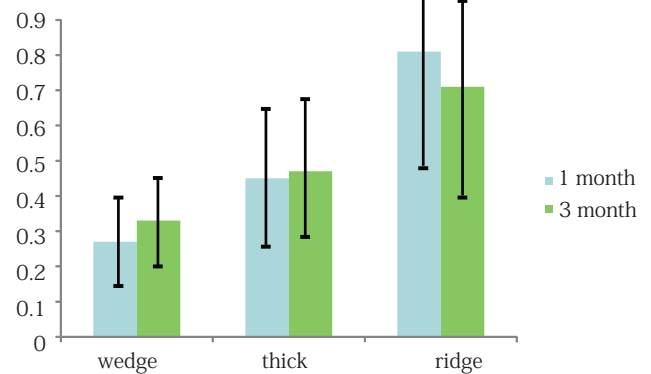
The RL-PIE of the wedge-type was $44.2 \pm 12.8\%$ at 1 month and $40.1 \pm 15.4\%$ at 3 months, which was not significantly different. The RL-PIE of the thick-type was $58.2 \pm 14.8\%$ at 1 month and $47.6 \pm 14.2\%$ at 3 months. The L-PIE at 1 months was significantly higher compared with 3 months ($P < 0.05$). The RL-PIE of the ridge-type was $64.6 \pm 12.7\%$ at 1 month and $58.8 \pm 14.4\%$ at 3 months. The L-PIE at 1 months was significantly higher compared with 3 months ($P < 0.05$). The RL-PIE of both the ridge-type and the thick-type were greater than the wedge-type ($P < 0.05$), and the ridge-type was more than the thick-type ($P < 0.05$). In other words, the PIE of the wedge-type was the shortest compared with the other two types.

4) W-PIE

(1) Top area (Fig. 7)



	1 month	3 months	$P < 0.05$
wedge	42.2 ± 12.8	40.1 ± 15.4	NS
thick	58.2 ± 14.8	47.6 ± 14.2	*
ridge	64.6 ± 12.7	58.8 ± 14.1	*



	1 month	3 months	$P < 0.05$
wedge	42.2 ± 12.8	40.1 ± 15.4	NS
thick	58.2 ± 14.8	47.6 ± 14.2	*
ridge	64.6 ± 12.7	58.8 ± 14.1	*

Fig. 6: RL-PIE

The RL-PIE of the wedge-type was not significantly different between 1 and 3 months. The RL-PIE of the thick-type was significantly greater at 1 month compared with 3 months ($P < 0.05$). The RL-PIE of the ridge-type was not significantly different at 1 and 3 months. The RL-PIE of both the ridge-type and the thick-type was greater than the wedge-type ($P < 0.05$) and the ridge-type was greater than the thick-type ($P < 0.05$).

Fig. 7: W-PIE at the top area

The W-PIE of the wedge-type at 3 months was significantly higher than at 1 month ($P < 0.05$). The W-PIE of the thick-type at 3 months was significantly higher than at 1 month ($p < 0.05$) just the same as the wedge-type. The W-PIE of the ridge-type was not significantly different between 1 and 3 months. The W-PIE of the wedge-type was significantly shorter than the thick- ($P < 0.05$) and ridge-types ($p < 0.05$) at each of the time periods.

The W-PIE of the wedge-type was 0.27 ± 0.12 mm at 1 month and 0.33 ± 0.11 mm at 3 months, which was significantly different ($P < 0.05$). The W-PIE of the thick-type was 0.45 ± 0.2 mm at 1 month and 0.47 ± 0.19 mm at 3 months, which was not significantly different. The W-PIE of the ridge-type was 0.81 ± 0.30 mm at 1 month and 0.71 ± 0.28 mm at 3 months. The W-PIE at 3 months was significantly less than at 1 month ($P < 0.05$). The W-PIE at the upper area of the wedge-type was significantly shorter than the thick-type ($P < 0.05$) and the ridge-type at each of the time periods.

(2) Middle area (Fig. 8)

The W-PIE of the wedge-type was 0.27 ± 0.14 mm at 1 month and 0.27 ± 0.09 mm at 3 months, which was not significantly different. The W-PIE of the thick-type was 0.50 ± 0.28 mm at 1 month and 0.46 ± 0.19 mm at 3 months, which was a significant difference ($P < 0.05$). The W-PIE of the ridge-type was 1.7 ± 0.61 mm at 1 month and 0.86 ± 0.19 mm at

3 months, which was a significant difference ($P < 0.05$). The W-PIE at the middle area of the wedge-type was significantly shorter than the thick-type ($P < 0.05$) and the ridge-type at each of the time periods. The W-PIE at the middle area of the thick-type was significantly shorter than the ridge-type at all time periods.

(3) Bottom area (Fig. 9)

The W-PIE of the wedge-type was 0.23 ± 0.09 mm at 1 month and 0.20 ± 0.04 mm at 3 months, which was not significantly different. The W-PIE of the thick-type was 0.66 ± 0.44 mm at 1 month and 0.35 ± 0.12 mm at 3 months, which was significantly different ($P < 0.05$). The W-PIE of the ridge-type was 1.36 ± 0.58 mm at 1 month and 0.46 ± 0.09 mm at 3 months, which was significantly different ($P < 0.05$). The W-PIE at the bottom area of the wedge-type was significantly shorter than thick-type ($P < 0.05$) and the ridge-type at each of the time periods. The W-PIE at the bottom area of the thick-type was significantly shorter than the ridge-type at all time periods.

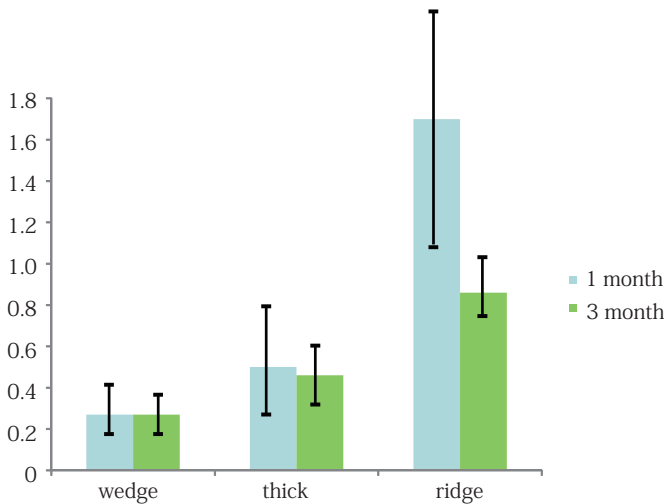


Fig. 8: W-PIE at the middle area

The W-PIE of the wedge-type was not significantly different between 1 and 3 months. The W-PIE of the thick-type at 3 months was significantly less than at 1 month ($p < 0.05$). The W-PIE of the ridge-type at 3 months was significantly less than at 1 month ($p < 0.05$). The W-PIE at the middle area of the wedge-type was significantly shorter than the thick- ($p < 0.05$) and ridge-types ($p < 0.05$) at each of the time periods. The W-PIE at the middle area of the thick-type was significantly shorter than at the ridge-type at all of the time periods.

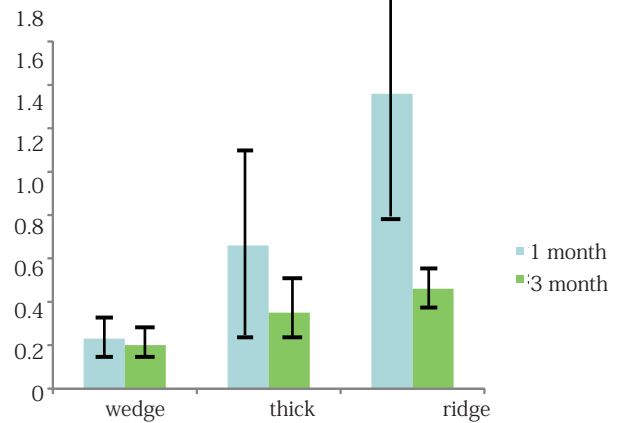


Fig. 9: W-PIE at the bottom area

The W-PIE of the wedge-type was not significantly different between 1 and 3 months. The W-PIE of the thick-type at 3 months was significantly less than at 1 month ($p < 0.05$). The W-PIE of the ridge-type at 3 months was significantly less than at 1 month ($p < 0.05$). The W-PIE at the bottom area of the wedge-type was significantly shorter than at the thick- ($p < 0.05$) and ridge-types at each of the time periods. The W-PIE at the bottom area of the thick-type was significantly shorter than at the bottom of the ridge-type at each of the time periods.

Discussion

1. Importance of the PIE

Dental implants lack structures that maintain the continuity of the epithelium by hemi-desmosomes and the basal lamina, which connect both the dental enamel and the attachment epithelium¹⁰⁾¹¹⁾. Dental implants create a lack of continuous epithelium because the oral mucosal epithelium is penetrated along the implant surface without hemi-desmosomes, and as a result, the PIE is formed⁴⁾. The L-PIE of the wedge-type was a similar length compared with the junctional epithelium, but both the thick- and ridge-types were much longer. Therefore, the PIE has a reduced capacity to act as a defense mechanism compared with the junctional epithelium, in terms of physical attachment, cell proliferating activity and lysosomal function⁶⁾⁷⁾. Moreover, the crevicular exudates continually wash the gingival sulcus through the intercellular space of the wider PIE in which the random migration of neutrophils help the phagocytes against invading pathogens³⁾.

Microbial plaque accumulations surrounding dental implants may develop into peri-implantitis, which is defined as inflammation or infection around an implant, with accompanying bone loss. Plaque accumulations are observed surrounding titanium implants, and many kinds of bacteria, which have been confirmed to be the same as periodontopathic bacteria¹³⁾, are recognized in the plaques. It is therefore important to prevent peri-implantitis and to create an ideal PIE which has a system of biological sealing. However, the morphological characterization of the PIE, in terms of elongation and thickness with time, has not been previously reported.

2. Morphological characteristics of the PIE

In 1997, Inoue et al. reported that turnover of the peri-implant is regulated by the basal cells and differentiates on the side of the implant surface in the same manner as the oral epithelium but not the attachment epithelium, which turns over both the inner and outer basement membrane sides and differentiates to the gingival sulcus⁸⁾.

This turnover prevents bacterial invasion of the attachment epithelium¹¹⁾. However, the thickness of the PIE is much less than the oral epithelium and the distribution of keratin filaments and the amount of PAS-positive protein is also less than the oral epithelium in dogs⁶⁾.

From the results of the histomorphometric analysis of this study, the RL-PIE of the wedge-type increased with time, but the thick- and ridge-types decreased with time. The W-PIE at the upper area of all groups was not significantly different with time but the ridge-type was much thicker than the others. The middle areas of the wedge- and thick-types were not significantly different with time, but the ridge-type was the thickest at 1 month, and decreased with time. Furthermore, the bottom area of the wedge-type was not significantly different but the thick- and ridge-types were thickest at 1 month and decreased with time. These results suggest that the wedge-type PIE is created but the disturbed inflammatory condition of connective tissue underneath the PIE creates the thick- and ridge-types of PIE. Once peri-implantitis occurs cell to cell adhesions might be destroyed and the infiltration of neutrophils and peeling of the PIE occurs allowing periodontal pathogenic bacteria to invade the connective tissue beneath the PIE. This would cause a collapse of PIE homeostasis and modify peri-implant tissues from the wedge-type to either thick- or ridge-types. Our results suggest that over 60% of an implant after implantation is usually under inflammation conditions and the PIE responds to these inflammatory reactions and creates the three types of shape. However, the PIE gradually becomes an ideal shape over time. This indicates that at the beginning of the implantation, avoiding inflammatory reactions is important and implant surface modification is necessary to prevent the accumulation of dental plaque and protect against bacterial invasion.

3. Improvement of peri-implant attachment

In this study, a milled polished surface implant was used. Inoue et al. 1987¹⁴⁾ reported that

cells migrate on the smooth surface but show contact guidance on a lined surface. Furthermore, they also reported that the extension and spread of both fibroblasts and epithelial cells are critically influenced by surface roughness and cells accumulate as a two center effect and stop the migration of the cells.

Cell migration is affected not only by surface roughness but also by large pore size. Our in vitro experiments also suggest that a large pore size of 50 to 100 μm is most critical for connective tissue cells to migrate into the pores and orient at right angles to the implant surface, similar to Sharpey's fibers. These oriented fibers might stop the migration of PIE cells. These surface topographies may help provide a biological seal around the implant¹⁵⁾.

As for the surface chemistry, methods of modifying the titanium surface using adhesive proteins such as osteonectin, fibronectin or laminin-5, which are compatible with the soft tissue/implant interface, have been proposed. The gingival epithelium attaches to dental implants through the formation of hemidesmosomes using laminin-5¹⁶⁾. Kokubun et al. reported that application of an artificial protein consisting of a mini-TBP motif and RGD motif creates a complete seal¹⁷⁾.

Conclusion

The PIE is divided in three types; the wedge-type is the most stable and these phenomena might be due to the degree of inflammatory reactions of the connective tissue after the implantation.

Acknowledgements

This research was partially supported by an Oral Health Science Center Grant 7 from the Tokyo Dental College and by the MEXT (Ministry of Education, Culture, Sports, Science and Technology) of Japan, 2010-2012.

References

- 1) Jung RE, Pjetursson BE, Glauser R, Zembic A, Zwahlen M, Lang NP: A systematic review of the 5-year survival and complication rates of implant-supported single crowns, *Clin Oral Implants Res*, 19: 119-130, 2008
- 2) Albrektsson T, Branemark PI, Hansson HA, Lindstrom J:

- Osseointegrated titanium implant, *Acta Orthop Scand*, 52: 155-170, 1981
- 3) Inoue T, Matsuzaka K, Yoshinari M, Tanaka T, Abiko Y, Shimono M: Current dental implant research, *Dentistry in Japan*, 41: 196-213, 2005
- 4) Klinge B, Meyle J: Soft-tissue integration of implants, Consensus report of Working Group 2, *Clin Oral Implants Res*, 2: 93-96, 2006
- 5) Bauman GR, Raley JW, Hallmon WW, Mills M: The peri-implant sulcus, *Int J Oral Maxillofac Implants*, 8: 273-280, 1993
- 6) Fujiseki M, Matsuzaka K, Yoshinari M, Shimono M, Inoue T: An experimental study on the features of peri-implant epithelium: Immunohistochemical and electron-microscopic observations, *Bull Tokyo Dent Coll*, 44: 185-199, 2003
- 7) Ikeda H, Yamaza T, Yoshinari M, Ohsaki Y, Ayukawa Y, Kido MA, Inoue T, Shimono M, Koyano K, Tanaka T: Ultrastructural and immunoelectron microscopic studies of the peri-implant epithelium -implant (Ti-6Al-4V) interface of rat maxilla, *J Periodont*, 71: 961-973, 2000
- 8) Inoue T, Takeda T, Chan YL, Abiko Y, Ayukawa Y, Tanaka T, Yoshinari M, Shimono M: Immunolocalization of proliferating cell nuclear antigen in the peri-implant epithelium, *Bull Tokyo Dent Coll*, 38: 187-193, 1997
- 9) Romanos GE, Schroter-Kermani C, Weingart: Healthy human periodontal versus peri-implant gingival tissue: an immunohistochemical differentiation of the extracellular matrix, *J Oral Maxillo Facial Imp*, 10: 750-758, 1995
- 10) Shimono M, Ishikawa T, Enokiya Y, Muramatsu T, Matsuzak K, Inoue T: Biological characteristics of the junctional epithelium, *J Electron Microsc*, 52: 627-639, 2003
- 11) Kinumatsu T, Hashimoto S, Muramatsu T, Sasaki, H, Jung H-S, Yamada S: Involvement of laminin and integrins in adhesion and migration of junctional epithelium cells, *J Periodontal Res*, 44: 13-20, 2009
- 12) Abrahamsson I, Berglundh T, Moon IS, Lindhe J: Peri-implant tissues at submerged and non-submerged titanium implants, *J Clin Periodontol*, 26: 600-607, 1999
- 13) Sumida S, Ishihara K, Kishi M, Okuda K: Transmission of periodontal disease-associated bacteria from teeth to osseointegrated implant regions, *Int J Oral Maxillofac Implants*, 17: 696-702, 2002
- 14) Inoue T, Cox JE, Pilliar RM, Melcher AH: Effect of the surface geometry of smooth and porous-coated titanium alloy on the orientation of fibroblasts in vitro, *J Biomed Mater Res*, 21: 107-126, 1987
- 15) Yoshinari M, Matsuzaka K, Inoue T, Oda Y, Shimono M: Bio-functionalization of titanium surfaces for dental implants, *Materials Transactions*, 43: 2494-2501, 2002
- 16) Tamura RN, Oda D, Quaranta V, Plopper G, Lambert R, Glaser S, Jones JCR: Coating of titanium alloy with soluble laminin-5 promotes cell attachment and hemidesmosome assembly in gingival epithelial cells: potential application to dental implants, *J Periodontal Res*, 32: 287-294, 1997
- 17) Kokubun K, Yoshinari M, Shiba K, Inoue T: Artificial proteins for functionalization of the surface of titanium implant, *Biomacromolecules*, 9: 3098-3105, 2008